The effect of bending on laser-cut electro-textile inductors and capacitors attached on denim as wearable structures

Pablo Escobedo[1], Jaime de Pablos-Florido[2], Miguel A. Carvajal[2], Antonio Martínez-Olmos[2], Luis F. Capitán-Vallvey[3], Alberto Palma[2, *]

[1] Bendable Electronics and Sensing Technologies (BEST) Group, Electronics and Nanoscale Engineering, University of Glasgow, Glasgow G128QQ, U.K.

[2] ECsens, Department of Electronics and Computer Technology, Sport and Health University Research Institute (iMUDS), University of Granada, 18071 Granada, Spain

[3] ECsens, Department of Analytical Chemistry, Excellence Unit of Chemistry applied to Biomedicine and Environment, Faculty of Science, Campus Fuentenueva, University of Granada, 18071 Granada, Spain

* Correspondence: ajpalma@ugr.es

Abstract:

In this paper we present the design, fabrication and characterization of electro-textile inductor and capacitor patterns on denim fabric as a basis for the development of wearable e-textiles. Planar coil inductors have been harnessed as antenna structures for the development of Near Field Communication (NFC) tags with temperature sensing capability, while interdigitated electrode (IDE) capacitors have been used as humidity sensors for wearable applications. The effect of bending in the electrical performance of such structures was evaluated, showing variations below 5% in both inductance and capacitance values for bending angles in the range of interest, i.e. those fitting to human limbs. In the case of the fabricated NFC tags, a shift in the resonance frequency below 1.7% was found, meaning that the e-textile tag would still be readable by an NFC-enabled smartphone. In respect of the capacitive humidity sensor, we obtained a minimum capacitance variation of 40% for a relative humidity range from 10% to 90%. Measured thermal shift was below 5% in the range from 10 to 40ºC. When compared to the 4% variation due to bending, it can be concluded that this capacitive structure can be harnessed as humidity sensor even under bending strain conditions and moderate temperature variations. The development and characterization of such structures on denim fabrics, which is one of the most popular fabrics for everyday clothing, combined

with the additional advantage of affordable and easy fabrication methodologies, means a further step towards the next generation of smart e-textile products.

Keywords: e-textile, denim fabric, planar coil inductor, interdigitated electrode capacitor, NFC tag, wearable electronics.

INTRODUCTION

There is a growing interest in the inclusion of electronic elements such as inductors and capacitors (targeted elements in this work), antenna structures, sensors and chips into fabrics to form compact and complete information systems integrated in clothing as wearable electronics.[1] This combination of electronics and textiles to form 'smart' textile products results in the so-called electronic textiles or e-textiles. Even though nowadays e-textiles still remains a sector in relative commercial infancy, studies indicate that the global smart textile market size is expected to reach $5,369 million by 2022 from $943 million in 2015, growing at an estimated compound annual growth rate (CAGR) of 28.4% from 2016 to 2022.[2] These information systems usually comprise of the following main components: sensors, actuators, data processing and energy management electronics, and communication antennas. The advantages offered by these systems are only surpassed by the technical challenges for their reliable fabrication, as the huge amount of related scientific articles makes evident.[3–8]. Among these challenges, the effects of mechanical strains such as bending or stretching on the embedded electrical components should be evaluated to ensure their correct operation when shaping to the human body.[9–11]

Recently, researchers have developed various types of textile antennas at higher frequency bands that realise off-body communications,[12] such as patch antennas applied in protective clothing for firefighters and basic attachments for standard clothes[13,14] and on jeans fabric.[15] Wearable ultra-high frequency (UHF) radio-frequency identification (RFID) antennas have also been developed and implemented on smart textiles for various applications, and the maximum read range is up to 16 m for patch UHF RFID antenna circuits with microchip connections.[16–18] Regarding conductive fabrics, textile conductors constructed by weaving,[19–21] knitting,[22] embroidering [23,10]

conductive threads or screen printed conductive inks could offer a suitable integration into the finished clothes.[9,10] However, a high packing density is challenging to achieve because of the lower mechanical flexibility of the conductive threads, and therefore, the embedded conductive patterns can exhibit low electrical conductivity for a high-performance antenna. Conventional woven fabrics coated with metal using an electro- or electroless plating method are simple in fabrication and provide sufficiently low sheet resistance and great mechanical flexibility.[24] Moreover, thermoplastic polymer-based conductive fabrics are generally compatible with laser cutting, and well defined and clean edges can be straightforward obtained.[25]

Different from UHF RFIDs, near field communication (NFC) systems have limited read range usually within a few centimetres, which are the best option in personal and high security applications such as debit/credit cards and facilities access cards. The operating frequency of an NFC antenna is typically set at 13.56 MHz, which corresponds to the high frequency (HF) range. A passive NFC tag is able to operate using the transmitted power from the RFID reader.[26] More interestingly, NFC tags can be read by any standard NFC-enabled smartphone.[27] Design methodology of e-textile wearable NFC antennas, material selections and embroidery techniques have been recently proposed and tested, showing suitable performance.[28] As a second element analysed, interdigitated electrode (IDE) capacitor is a well-known structure which has been attached to a great variety of substrates, including fabric for sensing purposes[29] and mainly in the form of supercapacitors for wearable energy storage.[30,31] Some examples of humidity capacitive textile sensors with a similar IDE topology can be found in the literature using different fabrication techniques such as inkjet-printing,[32] electroless plating,[33] weaving[34] or embroidery.[35] Its versatility, low energy consumption and low thermal drift make it a good choice to be integrated as sensor in fabric.

The influence of bending on wearable HF and UHF antennas has already been experimentally and theoretically analysed.[9–11,28] In most cases, although different fabrication techniques were employed, inductors and tags showed little variation of their electrical parameters, which leaded to proper operation with the only disadvantage of a shorter read range. Although significant efforts and remarkable advances have been achieved on this matter, more experimental tests and theoretical

discussion is still required to develop e-textiles on one of the most used fabric such as denim and focusing on affordable and easy fabrication methodologies, as well as adequate frequency communication bands for personal and/or high security applications.

In this study, we present two types of wearable electrical passive elements: planar spiral coil inductors as antennas for RFID tags in the HF band, and IDE capacitors as sensing devices of fabric moisture. Both components were designed and optimized in terms of size and performance by means of numerical simulation tools, and then fabricated using laser-cut silver-plated textile attached to 100% cotton denim fabric. Firstly, pattern spatial resolution study of this fabrication method was carried out as along with its physical characterization using 3D optical profilometry. Once minimal dimensions were verified to design compact elements, their electrical features were measured under bending strain conditions, to show their performance on non-flat surfaces. Finally, NFC tags were designed using the mentioned inductors, checking their resonance frequency, quality factor and functionality when read by an NFC-enabled smartphone.

MATERIALS AND METHODS

Design and transfer of electronic components on denim fabric

Electronic components (inductors and capacitors) were adhered to 100% cotton denim fabric with a thickness of 0.84 mm, which was purchased in a local textile store (Tejidos Buenos Aires, Granada, Spain). According to the literature, the relative permittivity for denim fabric (ε_r) is between 1.59 and 1.67.[36] Hereafter, an intermediate value of ε_r=1.65 was considered in numerical simulations. Inductors and capacitors were manufactured with silver conductive fabric (Ghiringhelli, Gallarate, Italy) with a thickness of 0.135 mm and a weight of 100 g/m^2. The metallization layer was made with galvanic deposit on all single polyamide yearns and then weaved. This process permitted to produce rip-stop polyester electric conductive fabric with high quality of electric and environment performances. According to the technical specifications provided in the manufacturer´s datasheet[37], this kind of conductive fabric provides stable low surface resistivity value (< 0.08 Ω/sq). The ESD Association Glossary[38] describes surface resistivity (also known as

surface resistance or sheet resistance) in the following way: “For electric current flowing across a surface, the ratio of DC voltage drop per unit length to the surface current per unit width. In effect, the surface resistivity is the resistance between two opposite sides of a square and is independent of the size of the square or its dimensional units”. Sheet resistance or surface resistivity is an electrical property used to characterise thin films with uniform sheet thickness. To avoid confusion with volume resistance (which is expressed in the units of Ω), sheet resistance is expressed in ohms per square (Ω/sq or Ω/□). The metallization process was made in respect to the last directives of RoHS 2.0 for the health and the environment protection from the risks of chemical substances. These cloths were made in compliance of flammability test as UL94 and rated as V0. Abrasion resistance is above 10^6 cycles. Manufacturer included a hot melt adhesive on the back side for adhesion on another surface. More technical specifications can be read on the manufacturer website.[39] Provided that its texture and flexibility are very similar to conventional fabrics, it was considered a promising candidate for developing wearable e-textiles.

The methodology for component design and transfer to the denim fabric was the following:

1. For designing and optimization purposes, numerical simulations of the electronic components were conducted with Advanced Design System (ADS software, Keysight Technologies, Santa Rosa, CA, USA) for inductances and COMSOL Multiphysics (COMSOL group, Stockholm, Sweden) for capacitors. Both simulation tools are based on a numerical discretization technique called the Method of Moments (MoM), which is used to solve Maxwell's electromagnetic equations for planar structures embedded in a multi-layered dielectric substrate.
2. Component patterns were designed using the Computer-Aided Design (CAD) software Inkscape 0.92.
3. Conductive textile was adhered to the denim fabric by heating with a home steam iron Ufesa PV1500 (B&B Trends, S.L, Barcelona, Spain).
4. Components were patterned on the adhered conductive textile by means of a Rayjet 50 laser engraver (Trotec Laser GmbH, Marchtrenk, Austria). This equipment is able to engrave, mark and cut a wide variety of materials with a CO_2 laser. Thickness and

material were configured together with power, velocity and resolution of engraving in order to cut the conductive top layer without damaging the denim fabric underneath.

5. Finally, excess conductive fabric was easily removed with tweezers, remaining the inductor or capacitor structures fully attached to the denim fabric.

The spatial resolution of this fabrication methodology was firstly evaluated with a pattern of parallel lines set with increasing width and gaps from 0.5 mm to 3 mm, as shown in Figure 1. As it can be observed, the thinners lines were not properly transferred. This experiment showed that 1.0 mm and 0.7 mm were the minimum line width and gap between lines respectively to obtain repetitive and reliable patterns. Compared to other conventional techniques such as embroidering and weaving, our methodology presented similar figures in terms of resolution (in the millimetre range) and possible cost. Other printing technologies such as inkjet or screen printing can provide more compact designs with resolutions in the range of micrometres.

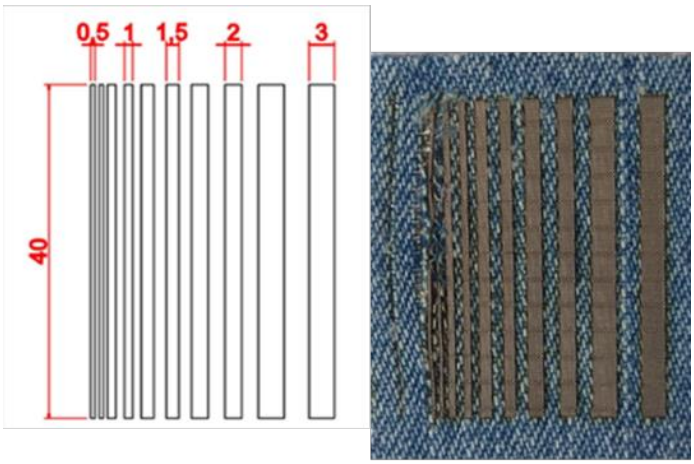

Figure 1. (a) Designed pattern for spatial resolution test where dimensions are given in mm, and (b) final transferred conductive pattern on denim fabric, showing incomplete lines under 1 mm width.

Design and fabrication of NFC tags and capacitor

As previously mentioned, the first example of application of this methodology for wearable electronics was to manufacture fully functional NFC tags on denim fabric. This wireless communication system comprises of two main parts: an antenna and a RFID chip. The system basically consists of a parallel LC resonant circuit whose resonance frequency, f_0, is given by:

$$f_0 = \frac{1}{2\pi\sqrt{LC}}, \quad (1)$$

where *L* is the inductance value given by the external antenna and *C* is the parallel capacitance needed to achieve resonance at the NFC frequency of 13.56 MHz. The RFID chip has an internal capacitance that is usually harnessed in the design of the inductance to obtain resonance at the desired frequency, thus avoiding the use of additional external capacitors. In this work, two NFC chips have been selected with different internal capacitances: SL13A (ams AG, Premstaetten, Austria) with C = 25 pF, and MLX90129 (Melexis, Ypres, Belgium) with C = 75 pF. Both NFC chips have in-built temperature sensors which can be read with an NFC-enabled smartphone. Using Equation 1 and the previous RFID chip internal capacitance values, the target inductance values were L = 5.5 µH and L = 1.84 µH for SL13A and MLX90129 chips, respectively. Because of the laser capability, squared designs were selected for the planar spiral coil inductors. Physical and electrical parameters of the substrate (denim fabric) and conductive textile were included in ADS software to design inductors with desired values and minimized dimensions. Optimized inductance patterns and complete tags are shown in Figure 2. A conductive bridge was also fabricated to connect both inductance ends to the NFC chip contact pads. Since this bridge has to go over the inductance, a non-conductive adhesive tape was stuck between them as shown in left pictures of Figure 2. Moreover, to strengthen the connection between the bridge and the inductance, conductive silver epoxy CW2400 (Chemtronics, Kennesaw, GA, USA) was applied. This epoxy was also used to attach the NFC chips.

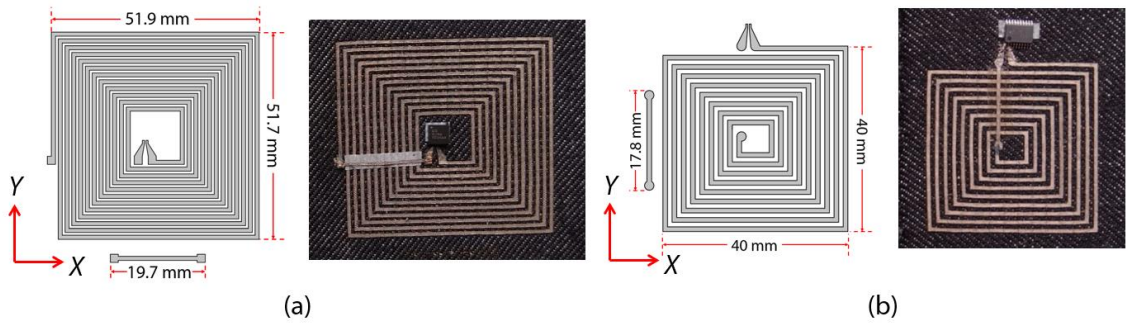

Figure 2. Designed inductive patterns and fabricated tags on denim fabric based on: (a) SL13A NFC chip and (b) MLX90129 NFC chip. Dimensions are given in mm.

As a second electronic component, an interdigitated electrode (IDE) capacitor was adhered to the denim fabric with the aim to use it as a wearable moisture sensor. In this case, design optimization was carried out with COMSOL software to achieve a capacitance value of 25 pF (as the internal capacitance of MLX90129 chip). Figure 3 shows the numerical simulation, designed pattern and fabricated capacitor.

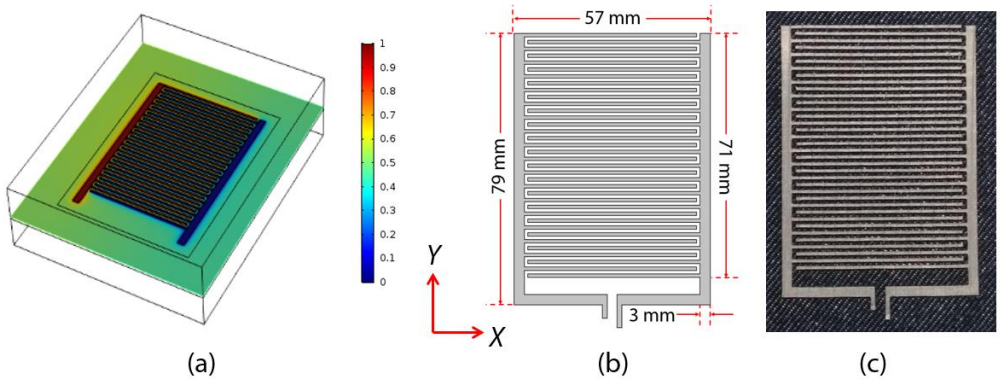

Figure 3. Designed 25 pF capacitor: (a) COMSOL simulation of electrical potencial, (b) designed pattern, and (c) fabricated capacitor on denim. Dimensions are given in mm.

Experimental setup

To study the effect of bending on the electrical performance of the designed components, the inductors and capacitors fabricated on denim fabric were bended by fitting them to the convex surfaces of hollow cardboard cylinders. Selected cylinder radii were 6.45, 3.55 and 3.10 cm. Three replicas of each structure were fabricated and

tested, showing results as the average values and error bars as standard deviations. For each component, the bending angle (α) in radians was calculated as its length in the curvature direction (L) divided by the cylinder radius (R), as depicted in Figure 4. Let us remember that a bending angle of $\pi/2$ represents that the component is covering a quarter of the full circumference length. In the case of the planar inductors, the bending was performed with respect to the square coil *Y* axes (see Figure 2). For the IDE capacitor, the bending study was performed along the axis parallel to the fingers' length. This direction was chosen because of the larger variation of distance between the electrodes. Physical characterization of the structures was carried out with a 3D optical profilometer S Neox (Sensofar S.A., Barcelona, Spain). 3D topography, dimensions and heights were measured with this equipment to check how the designed pattern is transferred to the attached components.

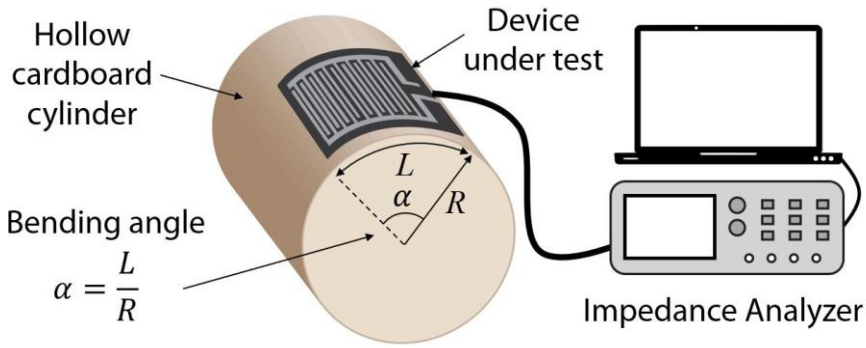

Figure 4. Experimental setup to study the effect of bending on the electrical performance of the designed components. As an example, an IDE capacitor is showed in the figure as the device under test.

With this setup, impedance measurements were performed with a 4294A Precision Impedance Analyzer (Keysight Technologies, Santa Rosa, CA, USA). To test the humidity sensing capability of the designed capacitor, the samples were placed inside a VCL4006 climate chamber (Weiss Technik, Reiskirchen, Germany). Relative humidity (RH) tests were done at 25ºC from 10% to 90% RH, waiting two hours between RH changes before gathering each capacitance measurement to ensure stabilized humidity. Moreover, the

temperature dependence was also measured between 10 and 40ºC at 40% RH with the climate chamber. To test the inductor performance, the Precision Impedance Analyzer was used to measure inductance, resistance and quality factor as a function of frequency at room temperature. The values of these parameters at the desired frequency of 13.56 MHz were extracted and showed as a function of the bending angle. Impedance as a function of frequency was also measured for the developed NFC tags, extracting the resonance frequency in each case. The influence of bending on this parameter was also analysed.

RESULTS AND DISCUSSION

Microscope image and profile of an inductor detail are displayed in Figure 5. The topography of the adhered conductive textile is shown with a measured thickness of 150 mm, close to the manufacturer specification. Trenches (deep blue in Figure 5B) were caused by the laser beam while was cutting. Moreover, dimensions of finger width (1 mm) and gap (0.7 mm) matches with the designed pattern.

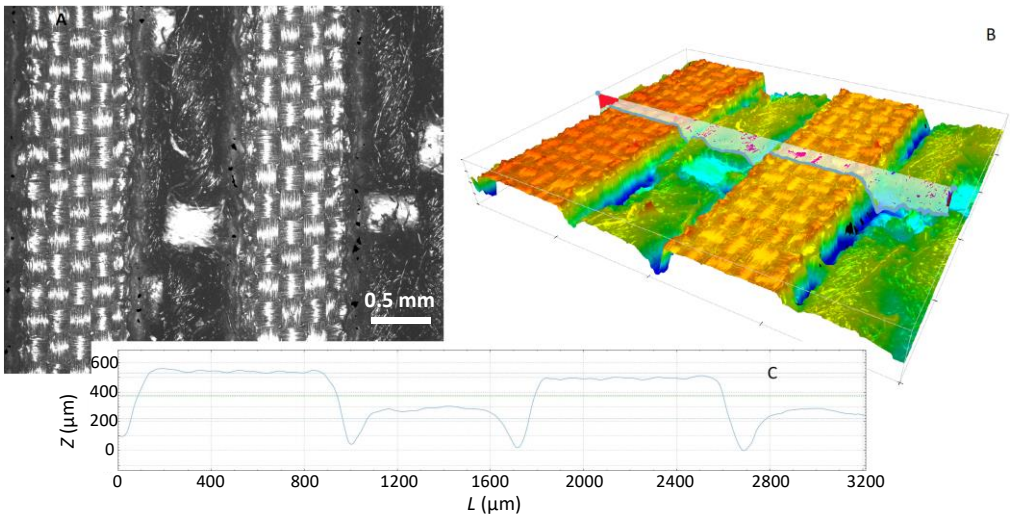

Figure 5. (A) 2D Microscope image of an adhered laser-cut inductor detail (two fingers) with magnification x5. (B) 3D pseudo-image from the profilometer showing e-textile (orange colour) and denim substrate (blue-green colours). (C) 2D profile of the structure by the line marked in (B).

Inductors and NFC tags

In Figure 6, electrical impedance of inductors (inductance and quality factor, Q) and complete NFC tags (impedance modulus and phase) of Figure 2 are shown as a function of frequency in flat position at room temperature. We can observe typical impedance figures as those obtained for these structures on rigid FR4 (substrate for printed circuit

At RF, an inductor is represented by the equivalent circuit model circuit[40] shown as insets in Figure 6. The main electrical parameter of the inductor that forms the antenna loop is the inductance L_a, which mainly consists of the mutual inductance due to coupling between the coil turns and some self-inductance due to the coil length[41]. In addition, there is also some parasitic resistance R_a to model the losses, and a parasitic capacitance C_a due to the electric coupling between the turns that contributes to a self-resonance. In fact, this causes the reactive part of the impedance to change over the frequency, as can be observed in Figure 6. At low frequencies close to direct current (DC) we can see an inductive behaviour. As frequency increases, reactive impedance varies to a frequency where it becomes zero, which is defined as the self-resonance of the antenna (f_{SR} in Figure 6). From that frequency onwards, the reactive part of the impedance adopts a capacitive behaviour. That is the reason why in Figure 6 the inductance value becomes negative, since a negative inductance can be seen as a capacitor that presents the same impedance as an inductor but with opposite phase. Therefore, it is necessary to operate sufficiently below the self-resonance frequency (in our case, 13.56 MHz) to ensure inductive behaviour.

A comparison between numerical and experimental data of results shown in Figure 6 at 13.56 MHz is displayed in Table 1. Excellent agreement between them is obtained, pointing out the reliability of the numerical simulations and the good electrical performance of the fabricated inductors.

Table 1: Averaged electrical parameters of inductors at 13.56 MHz.

NFC Chip	**SL13A**			**MLX90129**		
Parameter	*L* (µH)	*R* (Ω)	*Q*	*L* (µH)	*R* (Ω)	*Q*
Numerical	5.62	389	1.22	1.82	182	0.84
Experimental	5.61	326	1.46	1.82	160	1.02

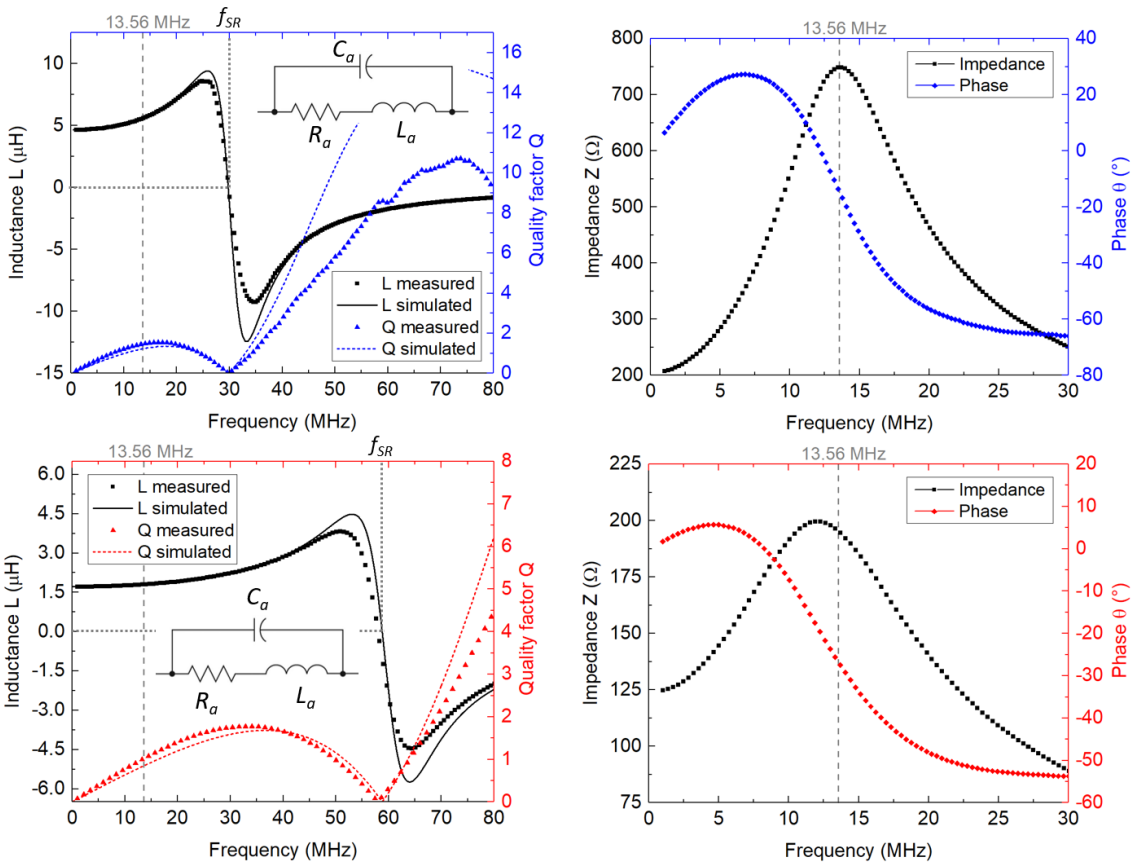

Figure 6. Upper charts: Inductance and quality factor of inductor and impedance NFC tag spectra for SL13A chip. Bottom charts: Inductance and quality factor of inductor and impedance NFC tag spectra for MLX90129 chip. Doted and solid lines show experimental data and numerical simulations, respectively.

Regarding the effects of bending on the electrical performance of these structures, inductance and quality factor *Q* of both fabricated inductors as a function of the bending angle are shown in Figure 7. A slight decreasing trend is shown in the inductance values, demonstrating the little effect of this bending in the studied range, which would be quite similar to the bending required for fitting to human limbs. However, it is worth mentioning that all the measurements have been taken off-body. We have measured inductances changes below 5% and of quality factor shift lower than 11% at 13.56 MHz. These trends have been previously experimentally observed and theoretically explained in similar structures.[42] In that work, the inductance decrease was attributed to a less efficient vertical magnetic flux creation through the centre of the inductor surface, thus

causing a negative effect in the mutual inductance due to a loss of flatness. When the antenna is no longer planar, the current flowing in the opposing sides of the inductor is closer to each other, thus the electromagnetic field exists on both sides of the element which tend to introduce extra electrical coupling that reduces the inductance value. In any case, these results show good performance robustness for the flexible inductors under mechanical bending strain.

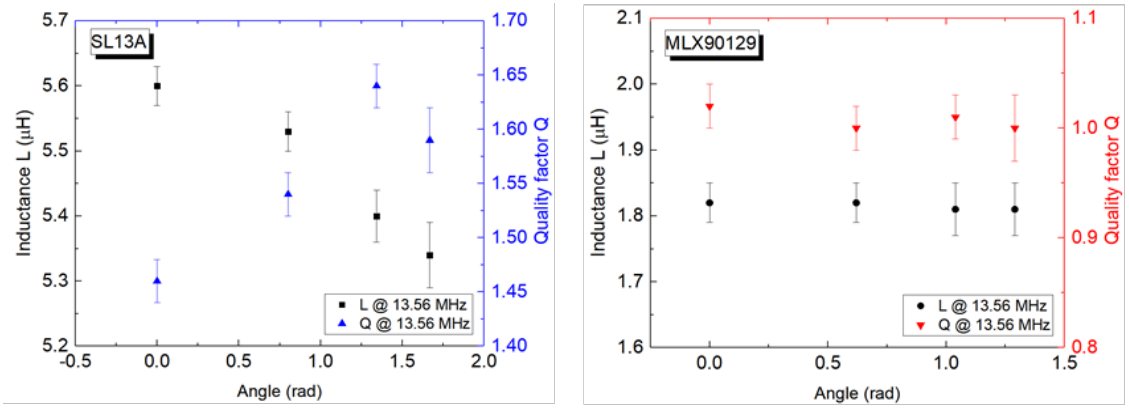

(a) (b)

Figure 7. Inductance and quality factor as a function of bending angle of inductors for (a) SL13A chip, and (b) MLX90129 chip at 13.56 MHz.

Moreover, the system reliability was also tested with the results showed in Figure 8, where the resonance frequency of the S13A tag versus bending angle is depicted. An average change lower than 1.7 % has been measured, providing correct reading out by the smartphone for all bended tags in the analysed range. This increasing tendency of the resonance frequency is consistent with the inductance decrease of Figure 7 considering Equation 1. Similar frequency shift has also been observed by Jiang et al for embroidered NFC antennas without affecting the tag operation either.[28]

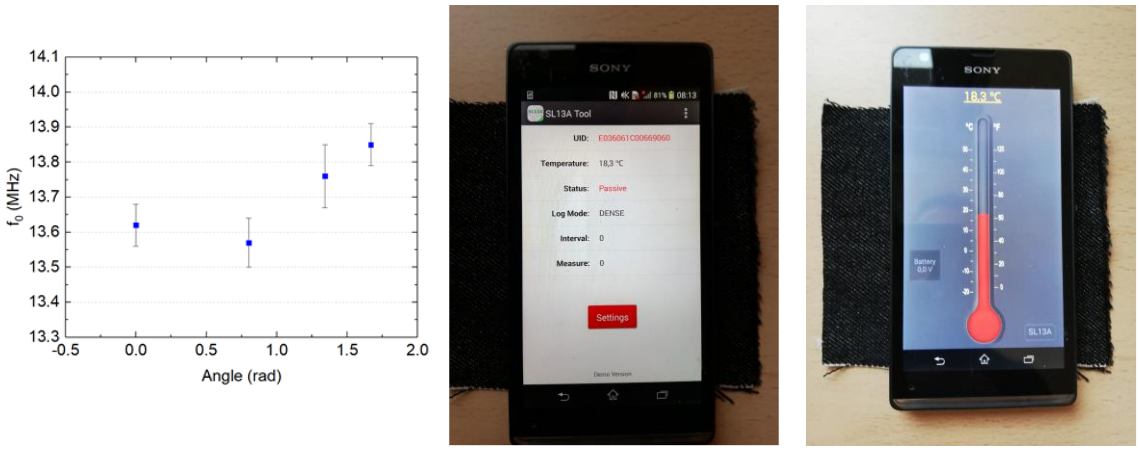

(a) (b)

Figure 8. (a) S13A tag resonance frequency vs. bending angle. (b) Pictures with screenshot of two SL13A-based apps showing tag reading and temperature measurement.

Capacitor

For the designed 25 pF capacitor of Figure 3, the experimental capacitance value of the developed capacitor was 23.0 pF at 13.56 MHz in flat position. In Figure 9, the effect of bending on the capacitance at this frequency is shown. No significant variations have been observed in the capacitance values at different frequencies as a function of the bending angle, therefore the 13.56 MHz has been maintained for potential compatibility with the HF band used in the NFC tags. According to Figure 9, a small increasing capacitance is measured with the increasing bending angle, observing a total change of 4%. This result can be explained with the study of Molina-Lopez et al,[43] who developed and experimentally validated a theoretical model of bended capacitive IDE structures. They modelled a capacitance whose value increased for outward bending, as we have obtained in this study. The coupling between electric field distortion and the geometrical changes on the devices due to bending strain have been proved to explain this effect.

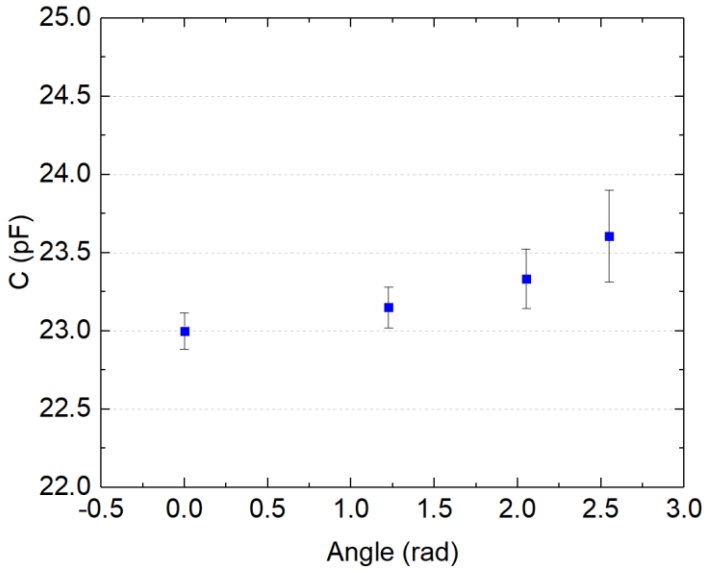

Figure 9. Experimental capacitance as a function of the bending angle.

In this study, we were also interested in the performance of the capacitor as humidity sensor. In this case, the cotton substrate will absorb surrounding water vapour with the consequent change in its dielectric constant and, as a consequence, in the capacitance of the interdigitated electrode structure. Experimental measurements of this electrical parameter as a function of the relative humidity have been conducted for different frequencies (i.e., 100 kHz, 1 MHz, 10 MHz and 13.56 MHz). The frequency of 13.56 MHz has been again maintained for potential compatibility with the HF band used in the NFC tags. From such measurements, an increasing linear trend is observed between 10% and 70% RH and a faster increase up to 90% for all cases. Therefore, each range can be fitted using the following trend curves:

$$C(pF) = a \cdot RH(\%) + b\,, (10\% \leq RH \leq 70\%\,) \quad (2)$$

$$C(pF) = a \cdot RH^2(\%) + b \cdot RH(\%) + c\,, (10\% \leq RH \leq 90\%) \quad (3)$$

Table 2 shows the obtained values for the parameters *a*, *b* and *c* in each case, as well as the coefficient of determination R^2. On the other hand, best sensitivity is obtained at the lowest tested frequency of 100 kHz, as already shown in previous works.[44,45]

Table 2: Experimental parameters for the fitting curves obtained for the two considered RH ranges in the study of the capacitance value as a function of RH at different frequencies.

***RH* range**	**Fitting curve parameter**	**100 kHz**	**1 MHz**	**13.56 MHz**
10% ≤ *RH* ≤ 70%	*a*	0.0188	0.0045	0.0014
	b	-1.1658	-0.2261	-0.045
	c	36.046	24.509	22.08
	R^2	0.9382	0.9711	0.9889
10% ≤ *RH* ≤ 90%	*a*	0.2128	0.108	0.0608
	b	19.106	20.316	20.783
	R^2	0.9049	0.9384	0.9617

Figure 10 represents the capacitance measurements at different frequencies as a function of the relative humidity. A range of capacitance variation from 250% to 40% has been obtained in the full range compared to the 4% due to bending. Therefore, this structure could be used as a humidity sensor even under bending strain conditions.

The double slope obtained depending on the RH range has also been observed in similar structures. Comparable capacitance curves for an IDE structure were found with a deposited layer of Nafion as sensing material.[44] The same behaviour was observed in ink-jet printed silver IDE capacitors on polyimide.[45] This tendency can be explained by the condensation of water on the sensor surface at high humidity levels, which could connect the electrodes and modify the global impedance.[46] Moreover, experimental hysteresis is below 3%, measured in relative humidity percentage. Therefore, the effect of humidity on cotton dielectric constant presents very similar behaviour to polymeric materials such as polyimide or Nafion.

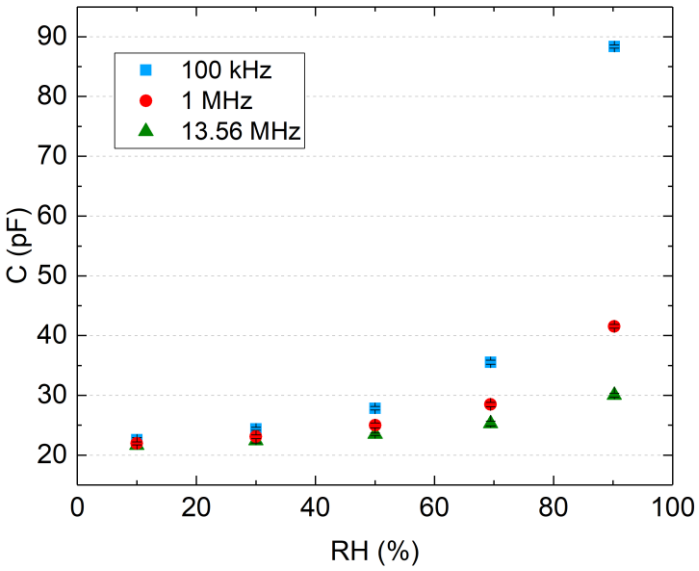

Figure 10. Capacitance versus relative humidity of the developed capacitors on denim fabric. Error bars are smaller than symbols.

Finally, the temperature dependence of the IDE structures was evaluated. To that end, three replicas were measured from 10 °C to 40 °C at an intermediate relative humidity value of *RH*=40 %. A linear temperature coefficient of α=1500±100 ppm was obtained, with R^2=0.979, resulting in a capacitance variation below 5% which is also much lower than the humidity dependence.

CONCLUSION

The growing interest of combining electronics and textiles to develop smart e-textile wearable devices is leading to the study on the performance of various electronic structures on fabric substrates. In this work we have fabricated some of the most interesting electronic patterns for the development of antenna structures and sensing devices, i.e. planar inductors and capacitors. Both pattern designs were simulated and optimized using specialised numerical simulation tools, and the resulting structures were attached using affordable and easy fabrication methodologies to denim fabric, which is one of the most used fabrics and therefore has a promising future for wearable electronics. On the one hand, the fabricated inductors were used as planar loop antennas in conjunction with two commercial RFID chips, thus obtaining wearable NFC

tags compatible with NFC-enabled smartphones. As a proof of concept, the tags were able to sense temperature thanks to the use of the on-chip temperature sensor. The tests carried out under different bending conditions demonstrated a change in the inductance value below 5% and below 1.7% in the resonance frequency. These results indicate that the e-textile device would still be readable by the smartphone for all bended tags in the studied range, which is similar to the required bending angles for fitting to human limbs. On the other hand, capacitive patterns were fabricated on denim fabric as humidity sensors by exploiting the interdigitated electrode structure and the change in the dielectric constant of the denim substrate with environmental humidity. A full-range variation between 250% and 40% in the capacitance value (at different frequencies) was obtained as compared to the 4% variation due to the bending effect. Temperature dependence of the capacitance provided a thermal shift below 5% in the analysed range. Therefore, this structure could be used as a humidity sensor even under bending strain conditions for the development of wearable e-textiles with potential applications in the fields of sports and fitness products or medical and healthcare devices for personal monitoring.

Declaration of conflicting interests

The authors declared no potential conflicts of interest with respect to the research, authorship, and/or publication of this article.

FUNDING

This study was supported by projects from the Spanish government (CTQ2016-78754-C2-1-R and EQC2018-004937-P). These projects were partially supported by European Regional Development Funds (ERDF). P. Escobedo wants to thank to the Spanish Ministry of Education, Culture and Sport for a R&D predoctoral grant (FPU13/05032).

REFERENCES

1. Shi J, Liu S, Zhang L, et al. Smart Textile-Integrated Microelectronic Systems for Wearable Applications. *Adv Mater* 2019; 1901958: 1–37.
2. Sharma K. Smart textile market overview, https://www.alliedmarketresearch.com/smart-textile-market (2017, accessed 17 December 2019).
3. Lam Po Tang S. Recent developments in flexible wearable electronics for monitoring applications. *Trans Inst Meas Control* 2007; 29: 283–300.
4. Salvado R, Loss C, Gonçalves R, et al. Textile Materials for the Design of Wearable Antennas: A Survey. *Sensors* 2012; 12: 15841–15857.
5. Park Y-GG, Lee S, Park J-UU. Recent progress in wireless sensors for wearable electronics. *Sensors (Switzerland)* 2019; 19: 1–34.
6. Stoppa M, Chiolerio A. Wearable Electronics and Smart Textiles: A Critical Review. *Sensors* 2014; 14: 11957–11992.
7. Occhiuzzi C, Cippitelli S, Marrocco G. Modeling, Design and Experimentation of Wearable RFID Sensor Tag. *IEEE Trans Antennas Propag* 2010; 58: 2490–2498.
8. Akbari M, Virkki J, Sydanheimo L, et al. Toward Graphene-Based Passive UHF RFID Textile Tags: A Reliability Study. *IEEE Trans Device Mater Reliab* 2016; 16: 429–431.
9. Virkki J, Björninen T, Merilampi S, et al. The effects of recurrent stretching on the performance of electro-textile and screen-printed ultra-high-frequency radio-frequency identification tags. *Text Res J* 2015; 85: 294–301.
10. He H, Chen X, Ukkonen L, et al. Textile-integrated three-dimensional printed and embroidered structures for wearable wireless platforms. *Text Res J* 2019; 89: 541–550.
11. Mukai Y, Bharambe VT, Adams JJ, et al. Effect of bending and padding on the electromagnetic performance of a laser-cut fabric patch antenna. *Text Res J* 2019; 89: 2789–2801.
12. Nepa P, Rogier H. Wearable Antennas for Off-Body Radio Links at VHF and UHF Bands: Challenges, the state of the art, and future trends below 1 GHz. *IEEE Antennas Propag Mag* 2015; 57: 30–52.
13. Hertleer C, Rogier H, Vallozzi L, et al. A Textile Antenna for Off-Body Communication Integrated Into Protective Clothing for Firefighters. *IEEE Trans Antennas Propag* 2009; 57: 919–925.
14. Chen SJ, Kaufmann T, Ranasinghe DC, et al. A Modular Textile Antenna Design Using Snap-on Buttons for Wearable Applications. *IEEE Trans Antennas Propag* 2016; 64: 894–903.
15. Gil I, Fernández-García R. Wearable GPS patch antenna on jeans fabric. *2016 Prog Electromagn Res Symp PIERS 2016 - Proc* 2016; 2019–2022.
16. Koski K, Syd??nheimo L, Rahmat-Samii Y, et al. Fundamental characteristics of electro-textiles in wearable UHF RFID patch antennas for body-centric sensing systems. *IEEE Trans Antennas Propag* 2014; 62: 6454–6462.
17. Virkki J, Wei Z, Liu A, et al. Wearable Passive E-Textile UHF RFID Tag Based on a Slotted

Patch Antenna with Sewn Ground and Microchip Interconnections. *Int J Antennas Propag* 2017; 2017: 1–8.

18. Ginestet G, Brechet N, Torres J, et al. Embroidered Antenna-Microchip Interconnections and Contour Antennas in Passive UHF RFID Textile Tags. *IEEE Antennas Wirel Propag Lett* 2017; 16: 1205–1208.

19. Xu F, Zhu H, Ma Y, et al. Electromagnetic performance of a three-dimensional woven fabric antenna conformal with cylindrical surfaces. *Text Res J* 2017; 87: 147–154.

20. Yao L, Qiu Y. Design and fabrication of microstrip antennas integrated in three dimensional orthogonal woven composites. *Compos Sci Technol* 2009; 69: 1004–1008.

21. Yao L, Qiu Y. Design and electromagnetic properties of conformal single-patch microstrip antennas integrated into three-dimensional orthogonal woven fabrics. *Text Res J* 2015; 85: 561–567.

22. Zhang S, Chauraya A, Seager R, et al. Fully fabric knitted antennas for wearable electronics. In: *2013 USNC-URSI Radio Science Meeting (Joint with AP-S Symposium)*. IEEE, pp. 215–215.

23. Gil I, Fernández-García R, Tornero JA. Embroidery manufacturing techniques for textile dipole antenna applied to wireless body area network. *Text Res J* 2019; 89: 1573–1581.

24. Guo L, Bashir T, Bresky E, et al. Electroconductive textiles and textile-based electromechanical sensors—integration in as an approach for smart textiles. *Smart Text their Appl* 2016; 657–693.

25. Haagenson T, Noghanian S, de Leon P, et al. Textile Antennas for Spacesuit Applications: Design, simulation, manufacturing, and testing of textile patch antennas for spacesuit applications. *IEEE Antennas Propag Mag* 2015; 57: 64–73.

26. Coskun V, Ok K, Ozdenizci B. *Near field communication : from theory to practice*, https://www.wiley.com/en-us/Near+Field+Communication+%28NFC%29%3A+From+Theory+to+Practice-p-9781119971092 (accessed 17 December 2019).

27. Escobedo P, Erenas MM, López-Ruiz N, et al. Flexible Passive near Field Communication Tag for Multigas Sensing. *Anal Chem* 2017; 89: 1697–1703.

28. Jiang Y, Xu L, Pan K, et al. e-Textile embroidered wearable near-field communication RFID antennas. *IET Microwaves, Antennas Propag* 2019; 13: 99–104.

29. Ataman C, Kinkeldei T, Mattana G, et al. A robust platform for textile integrated gas sensors. *Sensors Actuators, B Chem* 2013; 177: 1053–1061.

30. Muralee Gopi CVV, Vinodh R, Sambasivam S, et al. Recent progress of advanced energy storage materials for flexible and wearable supercapacitor: From design and development to applications. *J Energy Storage* 2020; 27: 101035.

31. Jia R, Shen G, Qu F, et al. Flexible on-chip micro-supercapacitors: Efficient power units for wearable electronics. *Energy Storage Mater* 2020; 27: 169–186.

32. Weremczuk J, Tarapata G, Jachowicz R. Humidity sensor printed on textile with use of ink-jet Technology. In: *Procedia Engineering*. Elsevier Ltd, 2012, pp. 1366–1369.

33. Li B, Xiao G, Liu F, et al. A flexible humidity sensor based on silk fabrics for human respiration monitoring. *J Mater Chem C* 2018; 6: 4549–4554.

34. Mattana G, Kinkeldei T, Leuenberger D, et al. Woven temperature and humidity sensors on flexible plastic substrates for e-textile applications. *IEEE Sens J* 2013; 13: 3901–3909.

35. Martinez-Estrada M, Moradi B, Fernández-Garcia R, et al. Impact of manufacturing variability and washing on embroidery textile sensors. *Sensors (Switzerland)*; 18. Epub ahead of print 8 November 2018. DOI: 10.3390/s18113824.

36. Sankaralingam S, Gupta B. Determination of dielectric constant of fabric materials and their use as substrates for design and development of antennas for wearable applications. *IEEE Trans Instrum Meas* 2010; 59: 3122–3130.

37. Ghiringhelli. Ghiringhelli EMI shielding, Conductive Cloths: EMI shielding fabrics, http://www.ghiringhellimario.com/content/file/catalogo/4_en.pdf (accessed 25 March 2020).

38. ESD. ESD Association Advisory for Electrostatic Discharge Terminology – Glossary of Terms ESD ADV1.0-2009. Revision of ESD ADV1.0-2004, http://www.esd-resource.com/userfiles/2011-05-19/201105190734531.pdf (accessed 25 March 2020).

39. Conductive Tissue - ghiringhellimario, http://www.ghiringhellimario.com/en/emi-products/conductive-tissue/ (accessed 17 December 2019).

40. Das S, Nguyen HL, Babu GN, et al. Free-Space Focusing at C-Band Using a Flat Fully Printed Multilayer Metamaterial Lens. *IEEE Trans Antennas Propag* 2015; 63: 4702–4714.

41. Gebhart M, Neubauer R, Stark M, et al. Design of 13.56 MHz Smartcard Stickers with Ferrite for Payment and Authentication. In: *2011 Third International Workshop on Near Field Communication*. IEEE, pp. 59–64.

42. Qin G, Liu H, Xu Y, et al. Characterization of flexible radio-frequency spiral inductors on a plastic substrate. *IEICE Electron Express* 2016; 13: 20160690–20160690.

43. Molina-Lopez F, Kinkeldei T, Briand D, et al. Theoretical and experimental study of the bending influence on the capacitance of interdigitated micro-electrodes patterned on flexible substrates. *J Appl Phys*; 114. Epub ahead of print 2013. DOI: 10.1063/1.4829023.

44. Weremczuk J, Tarapata G, Jachowicz RS. The ink-jet printing humidity sorption sensor-modelling, design, technology and characterization. *Meas Sci Technol*; 23, isi:000298240200007 (2012).

45. Rivadeneyra A, Fernández-Salmerón J, Agudo M, et al. Design and characterization of a low thermal drift capacitive humidity sensor by inkjet-printing. *Sensors Actuators, B Chem*; 195. Epub ahead of print 2014. DOI: 10.1016/j.snb.2013.12.117.

46. Sahm M, Oprea A, Bârsan N, et al. Water and ammonia influence on the conduction mechanisms in polyacrylic acid films. *Sensors Actuators B Chem* 2007; 127: 204–209.